Journal of
Marine Science and Engineering

MDPI

Article

Holocene and Reworked Pleistocene Sediments in Mud Depocenters of the Inner Continental Shelf of Sao Paulo Bight (Southeast Brazil)

Antonio Scardua Neto [1,2] and Javier Alcántara-Carrió [2,3,*]

[1] EGS Brasil, Av. Pedro Depiante, 115, Vitória 29075-150, Brazil; antonioscardua1@gmail.com
[2] Instituto Oceanográfico, Universidade de São Paulo, Praça do Oceanográfico, 191, São Paulo 05508-120, Brazil
[3] Department Geology and Geochemistry, Universidad Autónoma de Madrid, 28049 Madrid, Spain
* Correspondence: javier.alcantara@uam.es

Abstract: Mud depocenters are found across most siliciclastic continental shelves, occurring in various bathymetric ranges and typically dating to the Holocene. This study analyzes the sedimentary characteristics and formation processes of mud depocenters in the central sector of the inner continental shelf of the São Paulo Bight. A total of 1700 km of high-resolution seismic profiles, four gravity cores, and 1346 surface sediment samples were analyzed. The sedimentary analysis involved determining grain size parameters, organic matter content, carbonates content, and radiocarbon dating. Seafloor sedimentary mapping shows the predominance of very fine siliciclastic sand, together with three mud depocenters located shallower than the 30-m isobath. The northern depocenter comprises one sedimentary unit (SU-NZ-01), while the central depocenter consists of two sedimentary units (SU-CZ-01 and SU-CZ-02) and the southern depocenter is made up of two other sedimentary units (SU-SZ-01 and SU-SZ-02). Units SU-SZ-02, SU-CZ-02, and SU-NZ-01 were deposited on Precambrian rock surfaces during the Holocene transgression and include reworked sediments from nearby Upper Pleistocene coastal plains, characterized by a transparent seismic pattern. Above these, units SU-SZ-01 and SU-CZ-01 developed following the Holocene Transgression Maximum, associated with local mud input from the Peruíbe River mouth and the Santos Estuary, respectively. The paleorelief of Precambrian rocks favored the formation of these depocenters by creating wave shadow zones and trapping mud within the paleovalleys.

Keywords: grain size; cartography; sedimentary units; Holocene transgression

Citation: Scardua Neto, A.; Alcántara-Carrió, J. Holocene and Reworked Pleistocene Sediments in Mud Depocenters of the Inner Continental Shelf of Sao Paulo Bight (Southeast Brazil). *J. Mar. Sci. Eng.* **2024**, *12*, 2098. https://doi.org/10.3390/jmse12112098

Academic Editor: Markes E. Johnson

Received: 28 September 2024
Revised: 16 November 2024
Accepted: 18 November 2024
Published: 19 November 2024

1. Introduction

In most siliciclastic continental shelves, mud deposits are common features, characterized by distinct grain size, geometry, and internal sedimentary structures [1–5]. These mud deposits often form near river mouths, where there is a high input of mud sediments [1]. For example, along the northern coast of South America, the Amazon River discharges approximately 1150 × 10^6 tons of sediment per year into the Equatorial Atlantic Ocean [2], contributing to one of the largest mud deposits globally [3–5]. Although mud deposits are mainly associated with fluvial fine sediment input, these deposits can also occur in regions devoid of fluvial input, as that identified along the Gulf of Arguim (Mauritania), a region marked by high aridity where fine sediment input is mainly eolian [6]. A significant input of fine sediments is necessary for the development of mud deposits, but their location and formation also depend on other processes responsible for the control of sedimentation along marine environments, such as hydrodynamics, tectonic, and sea level oscillations, and the geomorphological setting [7]. From a hydrodynamic point of view, several pioneering models have already exposed the influence of waves, currents, and subsurface density flows on the transport and distribution of mud sediments along

continental shelves [8–10]. In general, the interplay between hydrodynamic and geomorphological factors (e.g., rock outcrops) determines the location of mud deposits. Sea level oscillations dictate the variations of accommodation space on continental shelves [11].

Research on mud deposits along continental shelves has grown in recent years, largely due to their environmental relevance. These deposits have a high capacity for adsorbing chemical pollutants, effectively acting as sinks for contaminants [12–15]. In addition, mud deposits also function as historical records of continental anthropic activities, as observed by Hanebuth et al. [16] when analyzing the levels of heavy metals along a mud deposit in the Bay of Cadiz (Spain). The interest in these deposits also lies in their possible sedimentological, stratigraphic, paleoclimatic and paleoceanographic implications [6,17–22].

This study aims to identify and characterize mud deposits along siliciclastic sediments on the inner continental shelf of São Paulo Bight (southeast Brazil), and to relate them to sea-level fluctuations.

2. Materials and Methods

2.1. Study Area

The study area is located in the central sector of São Paulo Bight (SPB), between the São Sebastião Channel and Peruíbe River mouth, down to 60 m depth (Figure 1). The SPB is an arc-shaped sector of the Brazilian continental shelf extending from Cape Frio to Cape Santa Marta [23]. Morphologically, the SPB varies in terms of width (70 km–230 km), slope (0.09°–0.04°), and depth of the shelf break point (120 m–180 m) [24]. The shelf is widest at the center, near the São Sebastião Channel, and becomes narrower and steeper in the north and south, near Cape Frio and Cape Santa Marta, respectively.

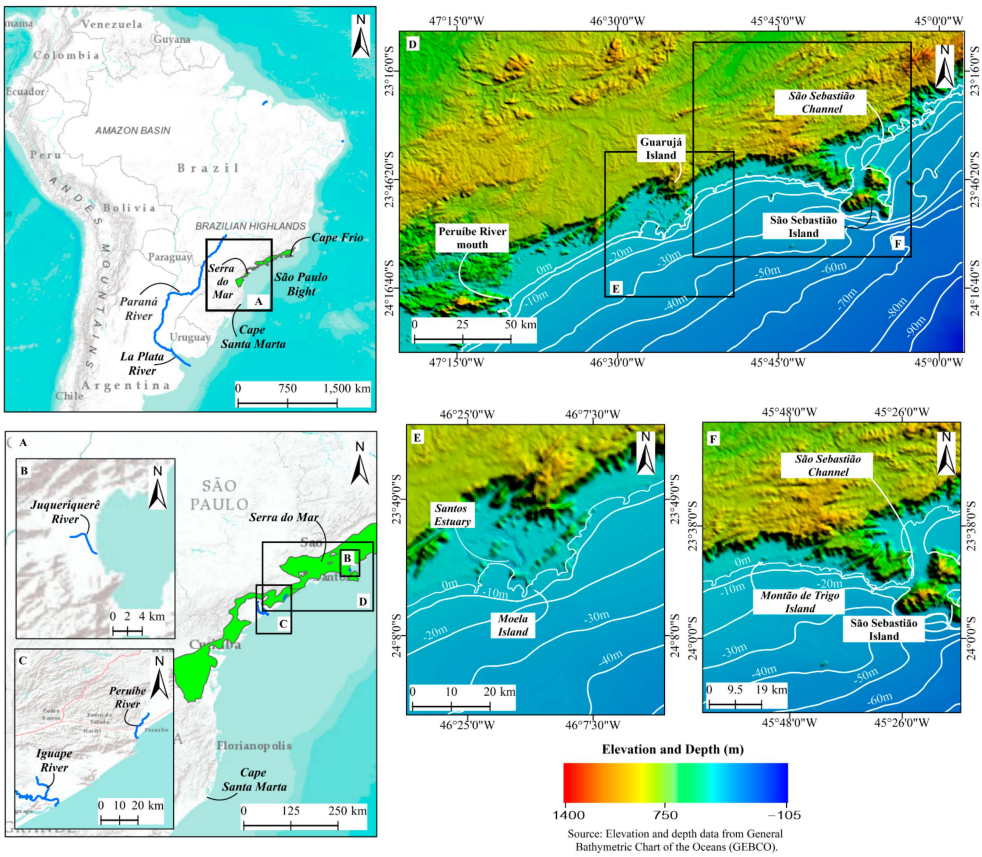

Figure 1. Location of the study area in the central sector of the inner continental shelf of São Paulo Bight (southeast Brazil). Location of the Sao Paulo Bight and Serra do Mar mountain range (A), the main rivers to the north (B) and to the south (C), the central zone of the Sao Paulo Bight (D), where the study has been carried out, and the main islands and other places cited in this study (E and F).

Santos Basin subsidence and Serra do Mar mountain range uplift since the Mesozoic determined the origin and main geological characteristics of the SPB [25]. However, the current geomorphology of the SPB is mainly controlled by the Late Quaternary Relative Sea Level Oscillations (LQRSLO) [26,27]. Between the Late Upper Pleistocene (120,000 years BP) and the present Holocene interglacial period, the Last Maximum Glacial (LMG) (18,000 years BP; 130 m below present mean sea level) was responsible for the exposure of the entire SPB to subaerial erosional processes, developing paleo-valleys that were then filled in during the Holocene [28].

As a consequence of the uplift of the Serra do Mar mountain range, most of the local fluvial courses near the SPB were diverted to the west and therefore, they began to contribute more significantly to the inland basins of the Parana and La Plata rivers [29]. Consequently, the direct supply of autochthonous terrigenous sediments to the SPB is low in the Holocene, thus contributing to the predominance of both relict sediments and modern allochthonous terrigenous sediments in the inner continental shelf. Current sedimentation rates in the continental shelf of SPB do not exceed 70 cm/ky, with the lowest values associated with high local hydrodynamics and low fluvial sediment input near both the Santos Estuary and the São Sebastião Channel [30].

The São Sebastião Island (SSI) marks the limit between two sedimentary provinces of the SPB with different grain size patterns of the seafloor. South of the SSI, where the study area is located, there is a predominance of sand along the inner continental shelf with an increase of mud towards the shelf break. In contrast, north of the SSI there are great heterogeneity, with mud patches interspersed with sand along the entire inner continental shelf [29,31–33]. Grain-size differences between these two provinces reflect the existence of distinct sediment sources and processes acting in each [29].

The local wind regime along the São Paulo shore is characterized by seasonality. During the austral spring and summer, winds blow mainly from the east and north, while during the austral autumn and winter, they blow mainly from southwest and west-southwest [34]. A local bidirectional current, induced mainly by the seasonality of the wind regime, flows parallel to the coast assuming a northeast direction during the austral winter and southwesterly during the austral summer [35]. This bidirectional pattern of the local coastal current, in association with the Coriolis force, induces specific dynamics in the local distribution of water masses. During the austral summer, these dynamics are based on the offshore surface displacement of the Coastal Water (CW) and Tropical Water (TW) together with the onshore sub-surface displacement of the South Atlantic Central Water (SACW); during the austral winter, the opposite occurs [36].

In addition to influencing the coastal current and water mass dynamics, the seasonality of the wind regime is also reflected in the local wave climatology. Under austral summer or winter winds conditions, there is a predominance of easterly or southerly waves, respectively; the latter, mostly associated with the cold fronts, are more energetic [37]. The region is characterized by a mixed microtidal regime [38]. Compared to the wind regime, tides show a weaker influence in the local hydrodynamics of the continental shelf hydrodynamic; their contribution to the local longitudinal and transversal fluxes is about 10% and 45%, respectively [39].

2.2. Data Acquisition, Processing and Analysis

Grain size distributions and carbonate content of 1346 surface sediment samples from the inner shelf were analyzed, in addition to approximately 1700 km of seismic profiles and 4 sediment cores. The carbonate content and grain size curves (obtained after destroying organic matter and carbonates) of the surface sediment samples were obtained from the database of the Brazilian Navy. Then, grain size parameters were computed by GRADISTAT 4.0 software [40] utilizing the formulae proposed by Folk and Ward [41]. Lastly, a sedimentary cartography of the seafloor was elaborated by ArcGIS software 10.5.

The seismic profiles and sediment cores were obtained after three oceanographic surveys directed by the authors aboard the oceanographic vessel Alpha Delphini between

2018 and 2019 (Figure 2 and Table 1). The seismic profiles were recorded by the use of a Chirp sub-bottom profiler system operating in low and high frequencies (2–8 kHz and 10–20 kHz). The MDCS Marine Geophysical Survey and Data Acquisition software 3.0 was used in this process, which allowed the simultaneous recording of low- and high-frequency seismic profiles. However, only the low-frequency profiles presented a satisfactory result for the proposed purposes of this study, with the high-frequency profiles not included in the results. The 4 sediment cores, in turn, were collected using a gravity corer system, positioned in strategic locations based on prior analysis of the seismic profiles.

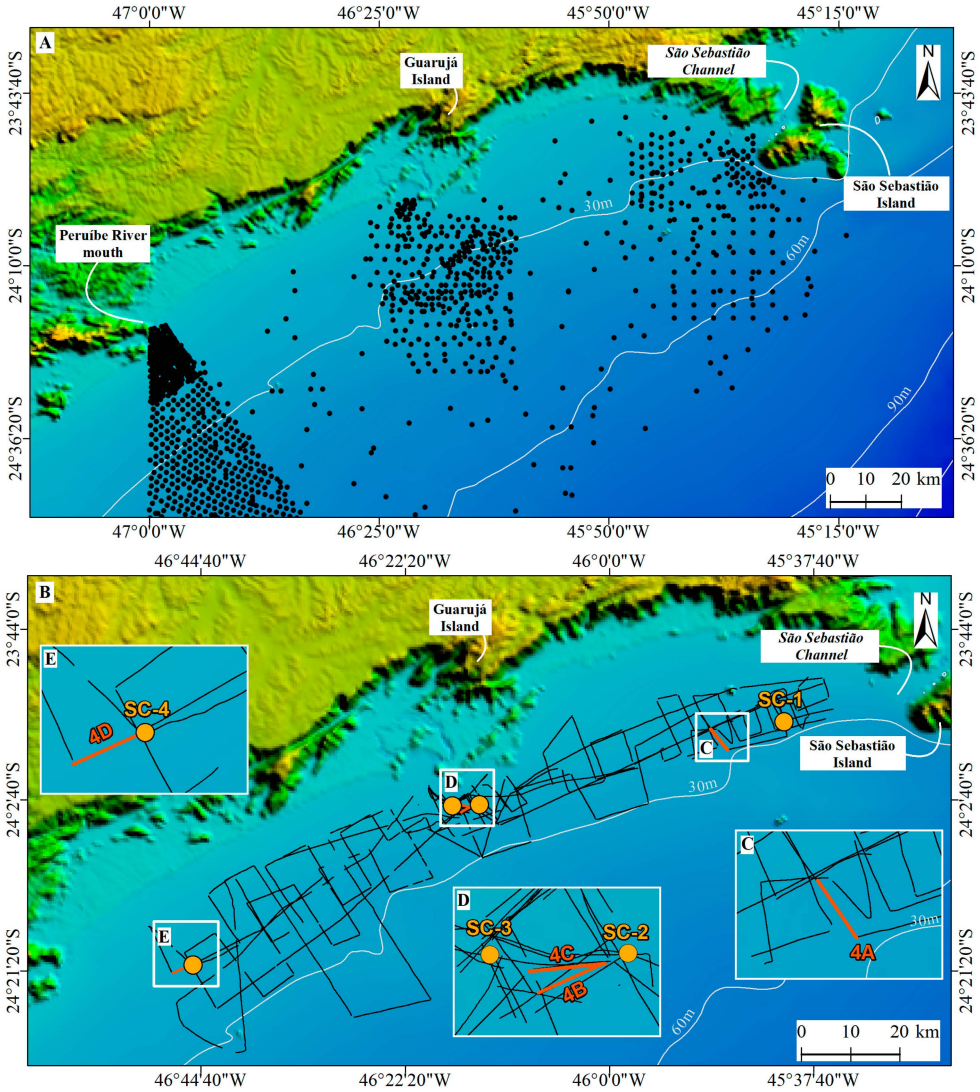

Figure 2. Location of the surface sediment samples (**A**), seismic profiles and sediment cores (**B**) analyzed, with the detailed location (**C**–**E**) of the seismic profiles shown in Figure 4.

Table 1. Location, depth (m below present mean sea level) and length (m) of the analyzed sediment cores.

Sediment Core	Latitude	Longitude	Depth	Length
SC-1	23°54′09.00″ S	45°41′00.30″ W	29.0	0.60
SC-2	24°03′23.28″ S	46°14′39.60″ W	19.2	1.55
SC-3	24°03′23.64″ S	46°16′48.30″ W	19.0	1.10
SC-4	24°20′45.18″ S	46°45′33.54″ W	21.5	1.26

The analysis of the low-frequency seismic profiles was conducted using the MDPS Data Processing and Interpretation software 3.0. The processing was based on offsets and filters applications, and main reflectors identifications. The identification of the reflectors allowed the delimitation of the respective sedimentary units, obtaining their horizontal and vertical distribution throughout the investigated area. The thickness of each mud unit was determined from the seismic profiles and mapped. When two overlapping mud units were identified, the total thickness was determined as the sum of thicknesses of both. However, it was not possible to obtain a good density of seismic profiles in the southern sector of the study area, and consequently, the map of thickness of the southernmost mud deposit could not be plotted.

The content of organic matter (OM) and carbonates of the sediment samples collected each 2 cm along the cores were determined following [42,43], and subsequently they were removed to carry out grain size analyses. The grain size distribution analysis was conducted by the sieving method [44] for the particles' size under 4 phi (very fine sand) and by the laser diffraction method for the particles' size over 4 phi. After, the main grain size parameters were calculated following the same methodology as described for the surface sediment samples. Also, the cores' samples were texturally classified using the ternary diagram proposed by Folk [45]. When relevant, calculations were performed to determine the mean, standard deviation and Pearson's correlation degree to better describe the results.

Four radiocarbon dating were realized on samples from the cores by the Accelerator Mass Spectrometry (AMS) method in the Beta-Analytic laboratories. For the dating, carbonated material at the cores' most basal samples were prioritized (SC-1: organic material, sampled at 0.58–0.60 m from sediments with mean size of very coarse silt; SC-2: fragments of bivalve mollusk shell sampled at 1.53–1.55 m; SC-4: organic material sampled at 1.24–1.26 m from sediments with mean size of medium silt). Due to the proximity of SC-2 and SC-3, only SC-2 was dated. An additional radiocarbon dating was carried out for a fragment of a bivalve mollusk shell sampled at 0.28–0.30 m of the SC-4. The dating' results were calibrated and corrected by both local ($\Delta R = 28 \pm 25$) [46] and global (IntCal13 or Marine13) reservoir effect [47].

3. Results

3.1. Seafloor Sedimentary Mapping

Approximately 99% of the area investigated is covered by sediments with a sand content greater than 50% (almost 82% of the area is covered by sediments with a sand content varying between 80 and 100%), while sediments with a total mud content greater than 50% only occur in about 0.85% of the study area. Despite this predominance of medium sand-sized sediment, there is an observed increase in total mud content both offshore (>60 m depth) and nearshore (<30 m depth), reaching a maximum of 76%, with silt content being higher than clay content. In addition, there are also some areas with a significant presence of gravel at medium depths (from 30 m to 60 m depth), reaching up to 39%, while 98% of the entire area has a gravel content of less than 10%. An increase in carbonate content is observed in these gravel patches, reaching up to 47%, while the rest of the area presents values below 10% (Figure 3A–F). According to grain size parameters, the seafloor surface is mostly covered by very well-sorted to moderately well-sorted sediment, with an average size of very fine sand. In contrast, areas with higher mud content are characterized by very poorly sorted or moderately poorly sorted sediment, with an average size of very coarse silt (Figure 3G,H).

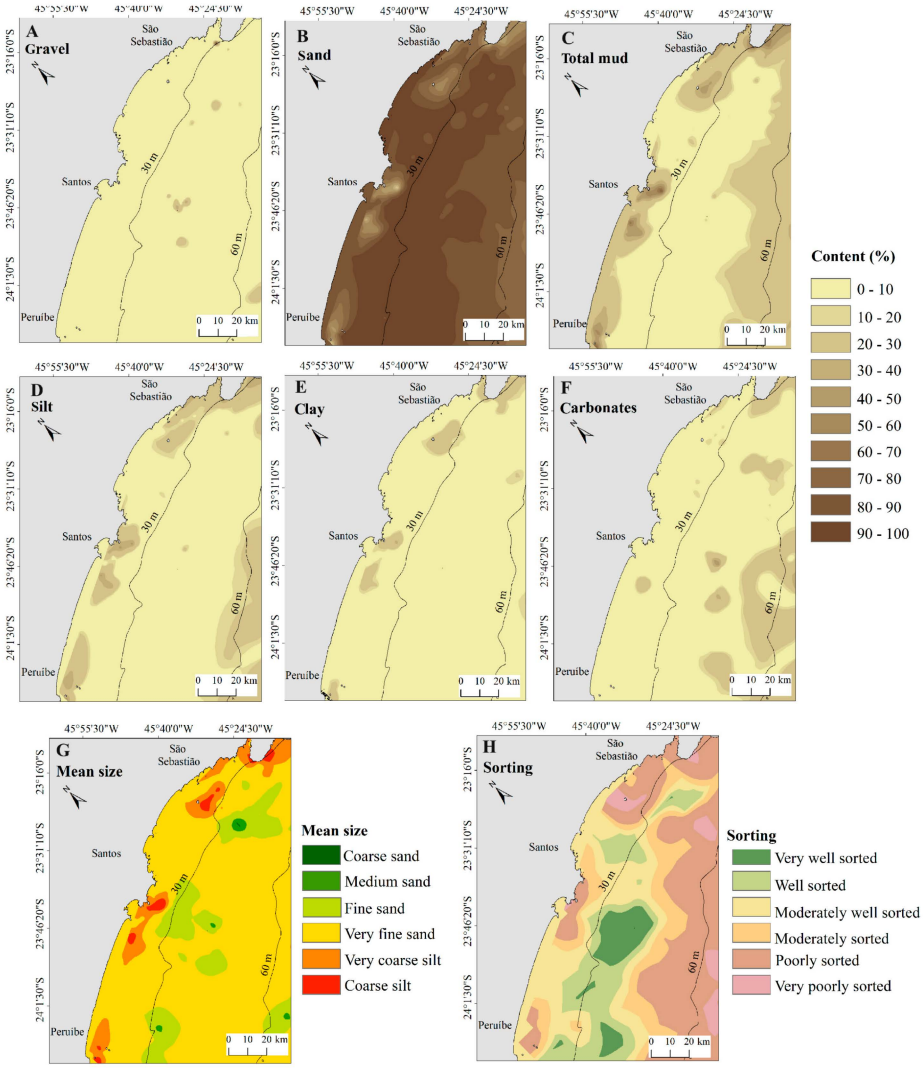

Figure 3. Sedimentary cartography of the seafloor along the central sector of São Paulo Bight (SPB), from the São Sebastião Channel to the mouth of Peruíbe River: percentage content of gravel (**A**), sand (**B**), total mud (**C**), silt (**D**), clay (**E**), and carbonates (**F**); mean size (**G**), and sorting (**H**).

3.2. Mud Deposits

Three mud depocenters were identified in the nearshore zone (<30 m depth) of the inner continental shelf (Figure 3G). The depocenter in the northern zone (NZ) is located around the island of Montão de Trigo, about 11 km from the south exit of the São Sebastião Channel and has an approximate area of 202 km^2 with a maximum lateral extension of 21 km. Like the NZ, the depocenter in the central zone (CZ) also occurs around an island, in this case, Moela Island, located south of Guarujá Island. This zone has, in turn, an area of almost 294 km^2 with an approximate extension of 38 km parallel to the coastline. Finally, the depocenter in the southern zone (SZ) occurs near the Peruíbe River mouth, with an approximate area of 149 km^2 and aligned parallel to the coastline for about 20 km.

The NZ depocenter is formed by a transparent seismic layer (SU-NZ-01) bounded at its base by an irregular surface with a high-amplitude reflector interpreted as the Precambrian rock surface (PRS) (Figure 4A). The CZ depocenter is characterized by the occurrence of a continuous high-amplitude reflector dividing two different seismic units, identified as SU-CZ-01 (upper) and SU-CZ-02 (lower) (Figure 4B). SU-CZ-01 presents low-amplitude internal reflectors, while SU-CZ-02 shows greater transparency with no occurrence of internal reflectors. Whenever present, SU-CZ-02 occurs below SU-CZ-01 and over the irregular and high reflectivity PRS. Both seismic layers occur concomitantly in the most central

portion of the CZ. In the absence of SU-CZ-02, SU-CZ-01 occurs at the most peripheral portions of CZ over a third layer (SU-CZ-03 characterized by the absence of seismic signal penetration (Figure 4C). The SZ depocenter contains two layers; SU-SZ-01 (upper) and SU-SZ-02 (lower) (Figure 4D). SU-SZ-01 is considerably thin and characterized by the occurrence of low-amplitude internal reflectors, while SU-SZ-02 presents greater thickness and transparency without the occurrence of internal reflectors.

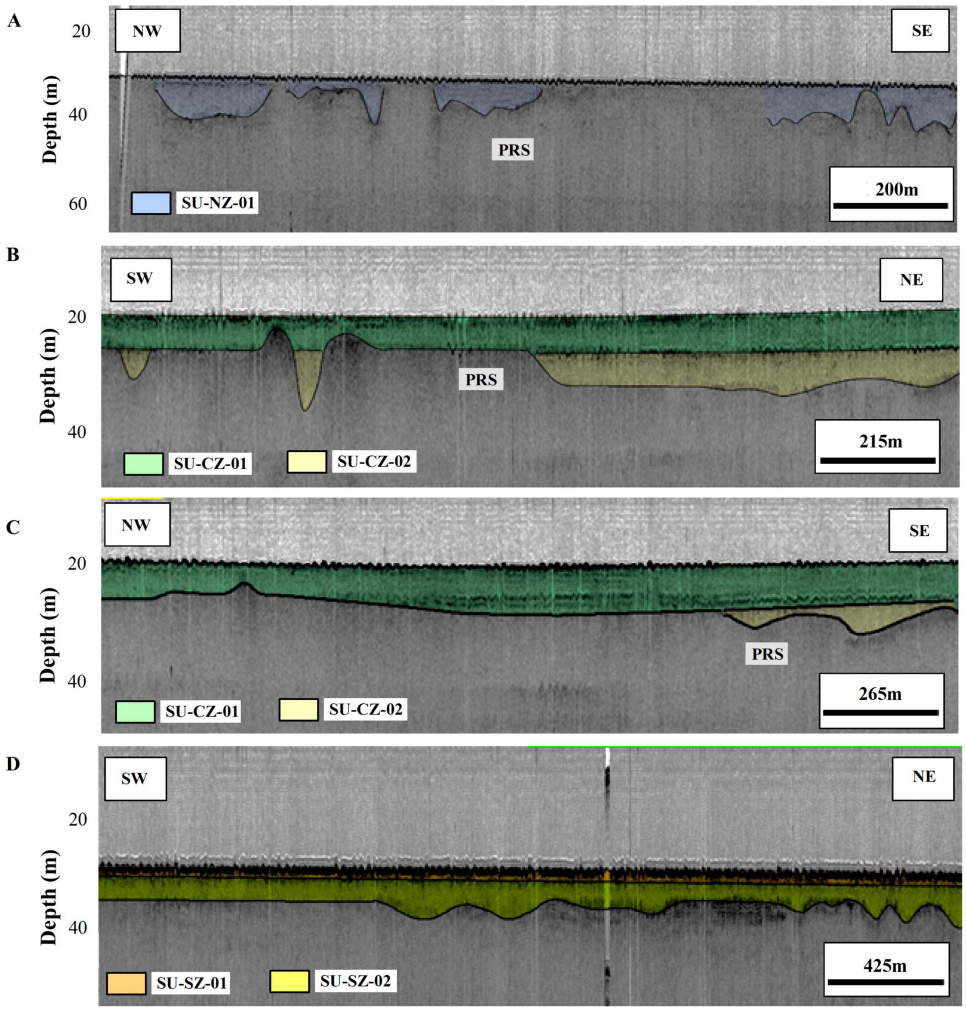

Figure 4. Identification of the seismic units (SU) via interpretation of the seismic profiles recorded along the mud depocenters in the Northern Zone (**A**), Central Zone (**B**,**C**), and Southern Zone (**D**).

The sediment thickness of SU-NZ-01 varies from 1.3 m to 10.3 m, with an average value of 5.2 ± 1.1 m (Figure 5A), mainly located at structural valleys of the irregular PRS. In turn, the sediment thickness of SU-CZ-01 ranges from 1.5 m to 12.3 m, with an average value of 5.2 ± 1.3 m (Figure 5B), while SU-CZ-02 presents sediment thickness ranging from 0 to 7.5 m and an average value of 0.8 ± 1.2 m (Figure 5C). Therefore, the total sediment thickness of the CZ mud deposit varies from 1.7 m to 19.8 m, with an average value of 6.0 ± 1.5 m (Figure 5D). The greatest sediment thickness extends radially from Moela Island, making it possible to identify the occurrence of a depocenter to the northwest of the island. The smallest thickness, in turn, is found along the most peripheral portions of the CZ, where SU-CZ-01 occurs over SU-CZ-03. Total sediment thickness along SZ reaches around 15 m, including SU-SZ-01 and SU-SZ-02. SU-SZ-01 is thinner than SU-SZ-02, being limited to only the first meters of the sedimentary record (up to 0.75 m near SC-4).

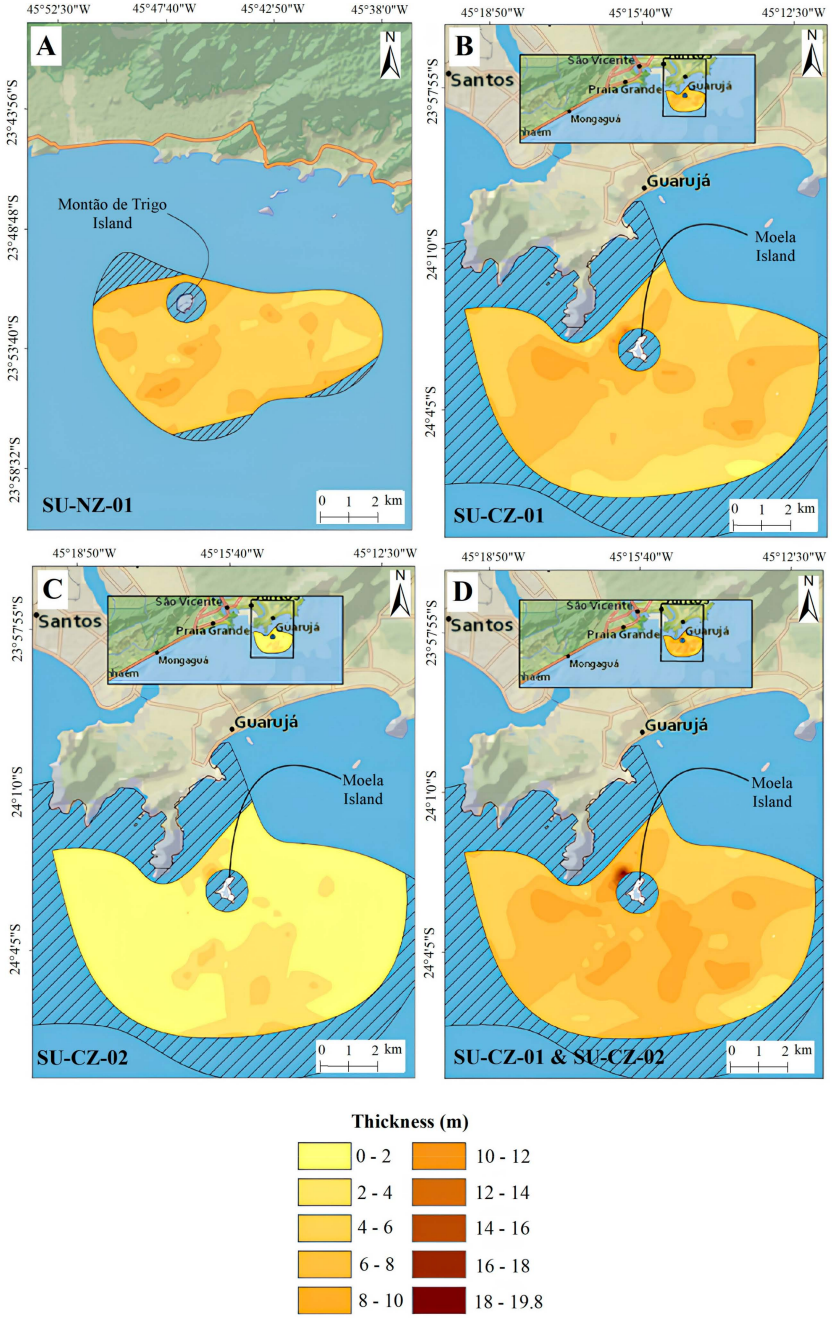

Figure 5. Sediment thickness of the sedimentary units SU-NZ-01 (**A**), SU-CZ-01 (**B**), SU-CZ-02 (**C**), and total sediment thickness of the Central Zone (CZ) (**D**). The hatched areas correspond to the zones with very coarse silt (see Figure 3G) without recorded seismic profiles.

The upper 0.60 m of SU-NZ-01 is composed of moderately to poorly sorted very fine sand and very coarse silt (Figure 6A) and is therefore texturally classified as silty sand (Figure 7A). Sand content (78.5 ± 7.0%) exceeds mud content throughout the entire sediment core SC-1, with silt content (20.5 ± 6.6%) being consistently higher than clay content (1.0 ± 0.5%) (Figure 8A). Despite the dominance of sand, an increasing trend in total mud content is observed in both the uppermost and basal sections, while the middle section shows a higher sand content. Organic matter content varied from 0.5% to 7.5%, averaging 2.6 ± 1.7% (Figure 6A). Higher values, found primarily in the upper section, decrease towards the base without significant correlation with other analyzed parameters. Carbonate content ranges from 3.2% to 23.1%, averaging 12.3 ± 5.6% (Figure 6A); it increases towards the middle section, similarly to the content of sand. Consequently, the mean size (phi units)

and carbonate content show a moderate negative correlation (r = −0.64), indicating a higher carbonate content for a coarser mean size of the sediments.

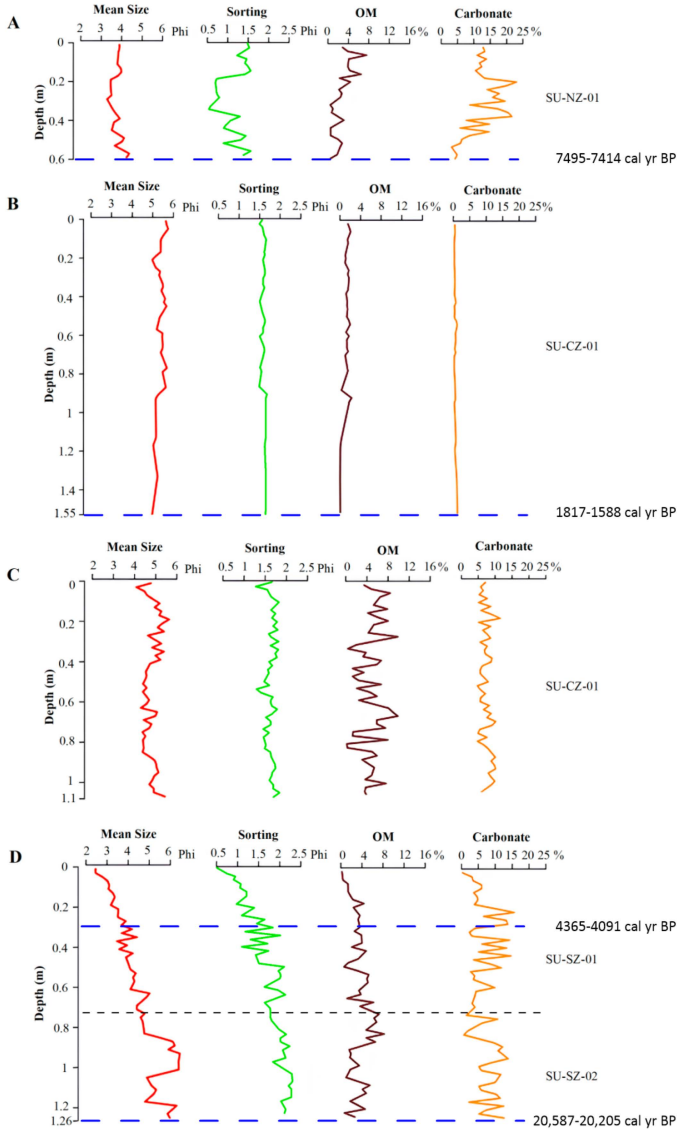

Figure 6. Vertical variations along the sediment cores of mean size, sorting, content of organic matter (OM) and content of carbonates, and position of the four radiocarbon dated samples. SC-1 (**A**) is representative of SU-NZ-01, SC-2 (**B**) is representative of the northern upper portion of SU-CZ-01, SC-3 (**C**) is representative of the southern upper portion of SU-CZ-01, and SC-4 (**D**) is representative of both SU-SZ-01 and SU-SZ-02.

The upper portion of SU-CZ-01 (up to 1.55 m) in the north is dominated by poorly sorted coarse to very coarse silt (sediment core SC-2, (Figure 6B), but in the south is dominated by poorly sorted very coarse silt to very fine sand (sediment core SC-3, (Figure 6C). Therefore, it is texturally classified as sandy silt (Figure 7B,C). Total mud content exceeds sand content to the north (69.4 ± 15%) (Figure 8B) and to the south (56.6 ± 12.7%) (Figure 8C). The content of silt and clay towards the north reach up to 90.4% and 4.0%, respectively, but coarser sediment is observed towards the south, where silt and clay contents reach up to 63% and 4.2%, respectively. The organic matter content varies from 6.9% to 16.0% (average value of 10.4 ± 1.7%) toward the north and from 0.2% to 9.8% (average value of 4.8 ± 2.4%) towards the south, while carbonate content varies from 0.3% to 13.5% (average value of 6.1 ± 3.4%) towards the north and from 4.8% to 11.4% (average value of

7.4 ± 4.8%) towards the south (Figure 6B,C). Therefore, an increase in organic matter and carbonate content is observed towards the north and south, respectively, but no significant correlation was obtained.

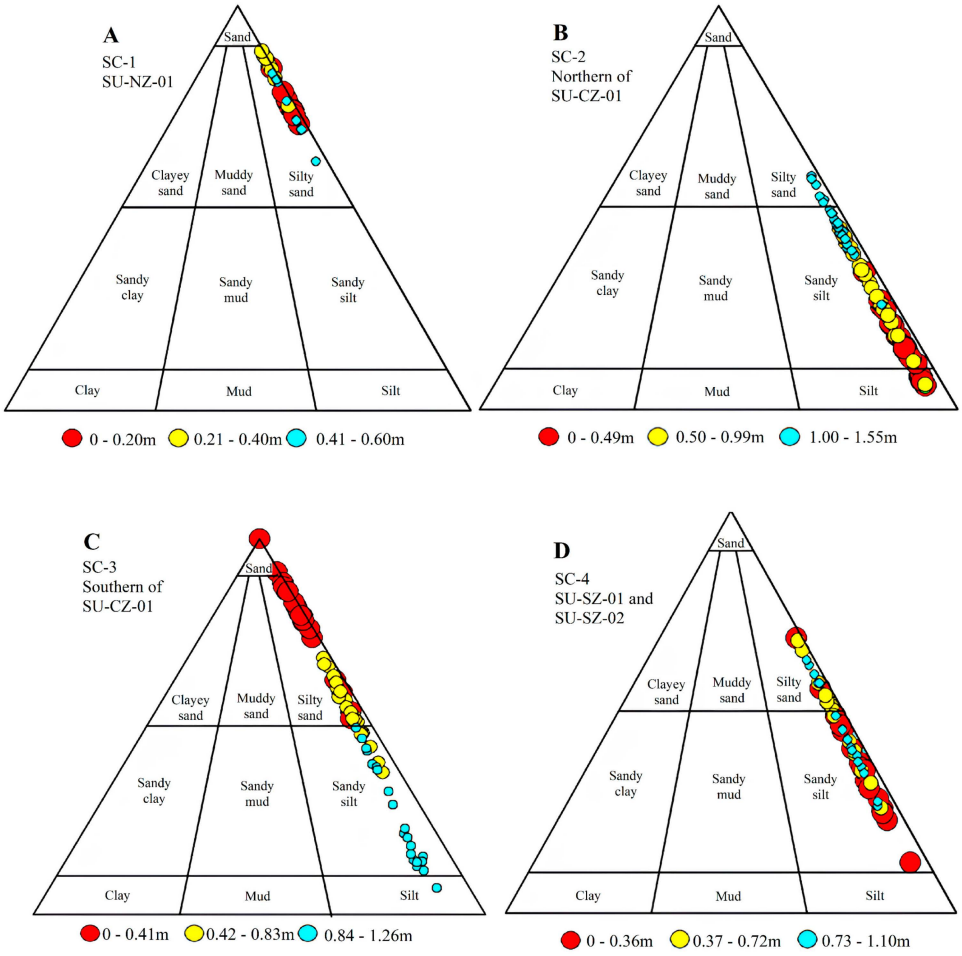

Figure 7. Classification of the core sediments after the ternary diagram of fine-grained textural classes of Folk (1954) SC-1 (**A**) is representative of SU-NZ-01, SC-2 (**B**) is representative of the northern upper portion of SU-CZ-01, SC-3 (**C**) is representative of the southern upper portion of SU-CZ-01, and SC-4 (**D**) is representative of both SU-SZ-01 and SU-SZ-02.

The SZ mud deposit shows a trend toward finer sediments. In fact, the upper 0.20 m of SU-SZ-01 is composed of moderately well-sorted fine sand (sediment core SC-4, Figure 6D), consequently texturally classified as sand (Figure 7D). At this 0.20 m layer, the sand content is at least 80%, reaching 100% at the upper 0.05 m, but below, the total mud content increases in a quasi-linear pattern, especially below 0.75 m, where SU-SZ-02 starts taking place. Thus, below 0.75 m, the mean total mud content reaches 70.1 ± 13.3%, with 64.3 ± 13.3% corresponding to silt and 5.8 ± 1.9% to clay (Figure 8D). Therefore, the upper sand layer is replaced by a layer composed of sandy silt and silt (Figure 8D), composed mainly of very poorly sorted coarse silt (Figure 6D). The OM content varies from 0.2% to 8.2% (mean value of 3.4 ± 1.8%) while carbonate contents vary from 0.4% to 15.59% (mean value of 7.0 ± 4.1%) (Figure 6D). A decreasing trend for the OM and carbonate contents is observed towards the top and bottom of the sedimentary record, but no significant correlation was found between these and the other two parameters.

The organic matter sample from SU-NZ-01 (taken at 0.58–0.60 m, bottom of the sediment core SC-1), along with the shells sampled from SU-CZ-01 (taken at 1.52–1.55 m, bottom of the sediment core-SC-2), and SU-SZ-01 (taken at 0.28–0.30, sediment core SC-4), have been dated to the Holocene period, with ages of 7454 (7495–7414), 1702 (1817–1588),

and 4228 (4365–4091) cal yr BP, respectively. In contrast, the sample of organic matter from SU-SZ-02 (taken at 1.24–1.26 m, bottom of the sediment core SC-4) has been dated to the Upper Pleistocene, with an age of 20,396 (20,587–20,205) cal yr BP (Figure 6 and Table 2).

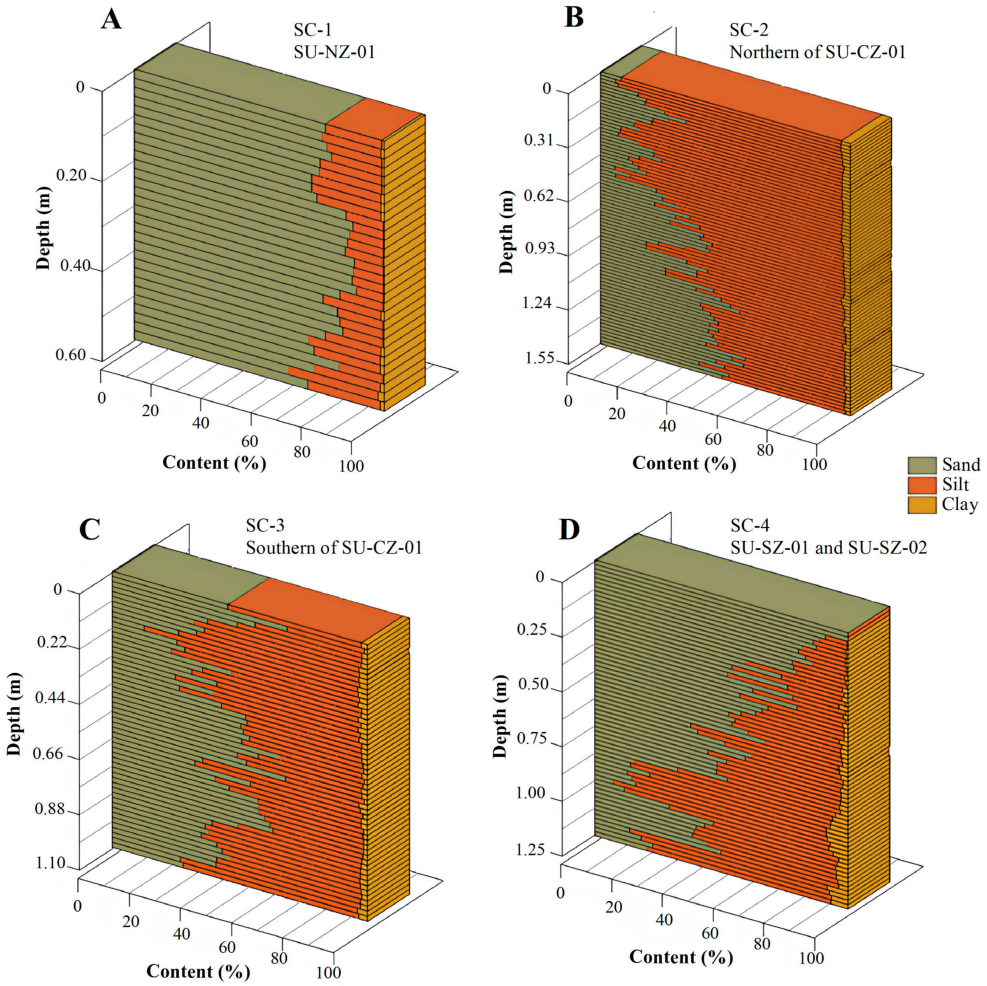

Figure 8. Sediment class distribution: percentages of sand, silt and clay along the sediment cores. SC-1, which is representative of SU-NZ-01 (**A**), SC-2, which is representative of the northern upper portion of SU-CZ-01 (**B**), SC-3, which is representative of the southern upper portion of SU-CZ-01 (**C**), and SC-4, which is representative of both SU-SZ-01 and SU-SZ-02 (**D**).

Table 2. Isotopic dating (cal yr BP) of samples of organic matter and shell fragments at different depths (m) from the cores corresponding to different seismic units.

Core	Depth	Dated Material	Seismic Unit	^{14}C Age
SC-1	0.58–0.60	organic matter	SU-NZ-01	7495–7414
SC-2	1.52–1.55	shell fragment	SU-CZ-01	1817–1588
SC-4	0.28–0.30	shell fragment	SU-SZ-01	4365–4091
SC-4	1.24–1.26	organic matter	SU-SZ-02	20,587–20,205

4. Discussion

4.1. Sedimentary Cover of the Seafloor

The central sector of the inner continental shelf of São Paulo Bight, from the São Sebastião Chanel to the Peruíbe River mouth, is mostly composed of very fine, well-sorted sand (Figure 3). This predominance of sandy sediments aligns with previous studies [29,31,48–52] and is attributed to the interplay between hydrodynamics and local

morphology. The coastline orientation, the arrangement of the isobaths, and the absence of major modifications in the seafloor relief induce a more effective action of southern waves [31,53]. These waves tend to remobilize an area extending from the coast to a depth of 50 m, with remobilization probabilities of silty sediment exceeding 50% [54]. Thus, it is inferred that mud sediment along the inner continental shelf of the SPB tends to be constantly eroded and transported elsewhere, contributing to the occurrence of high sand contents.

Lithoclastic sediments with a low carbonate content (≤10%) dominate the seafloor sedimentary cover. This low carbonate content is directly associated with local climatic conditions [31–33,54]. Although to a limited extent, an increase in carbonate content toward deeper areas was evidenced by the presence of isolated lithobioclastic deposits between 30 and 60 m depth. These isolated deposits compose a transitional zone preceding the deeper bioclastic one [33], and consist mainly of fragmented, gravel-sized relict shells [55], as depicted in the sedimentary cartography (Figure 3F). These gravel patches, with significant carbonate content, are relict in nature and thus have no implications for current hydrodynamics and sedimentary dynamics.

Similarly to the transitional lithobioclastic deposits, much of the identified lithoclastic sandy cover is also interpreted as relict, being composed mainly of coastal quartz sand eroded from the Pleistocene coastal plains during the Early Holocene marine transgression (Santos Transgression) [55,56]. Local hydrodynamic processes and biological activities act to rework the relict sandy cover [56]. Nittrouer et al. [57] point out that exposed and reworked relict sedimentary layers are characteristic of regions without relevant modern sediment input. This absence of modern sediment input along the inner continental shelf of São Paulo Bight is evidenced by low local sedimentation rates ranging between 2 and 68 cm/ky [30]. In comparison, such rates tend to reach up to 810 cm/ky in other portions of continental shelves off Brazil near significant fluvial systems [58]. Therefore, it can be inferred that the relict origin of the sandy sedimentary cover of the inner continental shelf of SPB, between the São Sebastião Channel and the Peruíbe River mouth, is directly associated with the scarcity of expressive fluvial sediment inputs. The Iguape and Juqueriquerê rivers are the main fluvial discharges to the São Paulo Bight, with approximately 435.0 m^3/s and 2.79 m^3/s, respectively [31,59], but they are located outside the study area. These values are very low compared to some other rivers that flow into the South American coast, such as the Paraíba do Sul River (1130 m^3/s) and the La Plata River (25,000 m^3/s) [60,61].

Although sandy sediments cover most of the investigated area, three mud depocenters have been identified (Figure 3). They are characterized by a mixture of sand, silt and clay, this mixture is found in most of the mud depocenters already identified along continental shelves worldwide [6,57,59,62,63]. Prior to this study, mud deposition had already been identified in some specific locations of the study area, such as near Santos Estuary [14].

4.2. Composition and Possible Sediment Sources of Mud Depocenters

Clay is present in the three identified mud depocenters, but its content levels never exceeded 9% (Figure 8). This low clay content was already expected, given that clay particles are preferably found in mud deposits near expressive rivers' mouths, such as those found along the Amazonian and Uruguayan continental shelves associated with the Amazon and La Plata rivers, respectively [64,65].

The total mud content in the NZ depocenter is lower than the sand content (Figure 8A). This pattern has been previously identified in other depocenters and is directly related to a decrease in silt and clay contents towards the lateral boundaries of the deposits [63,66]. A similar variation is also observed in the CZ depocenter, where SC-2 and SC-3, located approximately 3.5 km apart, indicated a trend of sediment thinning to the north, within the deposit's boundaries (Figure 8B,C), probably associated with local hydrodynamic conditions.

Like the sandy sedimentary cover, the identified mud depocenters are also composed of lithoclastic sediments, with very low carbonates content (Figures 3F and 6), similarly to other shelves [67]. The presence of lithoclastic sediment on continental shelves is

commonly attributed to fluvial discharges, since 90% of the sediment load of rivers consists of terrigenous muddy sediments [57,64,68–72]. Despite the absence of significant fluvial inflows along the continental shelf examined, [31] identified the influence of minor river courses contributing to the input of fine sediment and organic matter north of the São Sebastião Island. Furthermore, Vieira et al. [59] also confirmed the significance of this sediment source in supplying muddy sediments to the region, and they were also identified in a near coastal tidal flat within the São Sebastião Channel [73]. Therefore, despite their limited contribution, the role of small local fluvial systems in delivering muddy sediments to the studied inner continental shelf cannot be completely ruled out, especially during the austral summer when the coast of São Paulo experiences its highest precipitation rates.

In the assessment of the three identified depocenters, it is notable that both the CZ and SZ deposits are located near river mouths, suggesting that the sediment loads from these rivers could contribute significantly over time to the formation of these deposits. In contrast, the NZ deposit is not close to a river mouth, but mud may be supplied to the area by the São Sebastião Channel, which transports sediment through its southern mouth during fair weather conditions [74].

4.3. Controlling Factors of Mud Deposition

Once supplied to the marine environment, fine sediments are transported long distances until they settle. Near São Sebastião Island, the landward movement of Coastal Water during the summer, together with the meandering of the Brazil Current, greatly increases the transport of suspended sediment to the outermost region of the continental shelf. This process facilitates the deposition of mud at greater depths [53].

In the central portion of the investigated area, near Santos Estuary, Coelho [75] observed that the extensive rock outcrop (Moela Island) creates a wave shadow zone between the island itself and the mainland. Within this zone, there is a marked reduction in significant wave height, approximately 60% less than the rest of the shelf. This sheltered zone promotes the deposition of fine sediments, especially during the passage of cold fronts, when an advection of the sediment plume from the Santos Estuary towards the island is observed. The reduction in hydrodynamic conditions due to rock outcrops has been verified further north of the study area. Thus, Vieira et al. [59] observed that under easterly wave conditions, São Sebastião Island tends to create a wave shadow zone towards the south of the island, promoting the deposition of muddy sediments. Thus, the association between hydrodynamics, morphology, and the output of muddy sediments through the southern mouth of the São Sebastião Channel in fair weather conditions can favor the supply and deposition of mud in the vicinity of Montão de Trigo Island, located around 25 km south the São Sebastião Channel.

Reduced hydrodynamics within the sheltered zones also facilitate organic matter deposition, since its settling velocities is similar to that of mud particles [76]. Selective deposition of organic matter in low-energy zones has been documented in several environments near the study area, including the Santos Estuary [77], the São Sebastião Channel [78], and Ubatuba Bay [79].

Rock surfaces, in addition to creating wave shadow zones, influence the thickness of mud deposits. Thus, mud deposits tend to fill paleovalleys. The control of rock surfaces on the location of mud deposits has been recognized elsewhere, including the Portuguese continental shelf [80] and the Escagerraque Strait in Norway [81]. According to Hanebuth et al. [11], these deposits are classified as Mud Entrapments, characterized by their occurrence at the boundaries of elevations and depressions, where sediment entrapment is a recurrent phenomenon.

4.4. Mean Sea Level Conditions for Formation of Mud Deposits

The absence of sedimentary record between the Quaternary mud deposits and the Precambrian rock surface suggests that, during the previous sea-level fall, up to the LMG, the older sedimentary layers were eroded, exposing the rock basement. The subsequent

sea level transgression led to the filling of the accommodation space, forming the identified mud deposits. A similar process was documented in Guanabara Bay, where intense mud deposition occurred during the Holocene marine transgression covering both the thin layer of Pleistocene fluvial sands and the Precambrian rock surface [82].

The lower sedimentary units of the CZ (SU-CZ-02) and SZ (SU-SZ-02) depocenters, as well as the only sedimentary unit of the NZ (SU-NZ-01) depocenter, show transparent seismic patterns. Transparent seismic units have been interpreted as sediments with homogeneous settling velocity and density [83] and have been described in continental shelf environments as forming during sea level transgressions and/or highstands [84]. These sedimentary units with transparent seismic patterns have been described as filling incised valleys during the Early Holocene transgression within in the LMG [85–87]. Therefore, it can be deduced that Pleistocene sediments from the coastal plains of São Paulo Bight were reworked during the Holocene transgression, in accordance with [54,55], forming the transparent seismic unit of the inner shelf that has been identified in the lower part of the SZ (SU-SZ-02). Thus, although the organic material of the sediment from SU-SZ-02 has an age of 20,396 (20,587–20,205) cal yr BP (Table 2), the reworking of these Pleistocene sediments and deposition of the SU-SZ-02 should occurred during the Holocene transgression, similarly to SU-NZ-01, which has similar seismic characteristics and an age of 7454 (7495–7414) cal yr BP, and SU-CZ-02. SU-NZ-01 formed during the Holocene transgression, while SU-CZ-01 and SU-SZ-01 formed after the HMT (Figure 9 and Table 2).

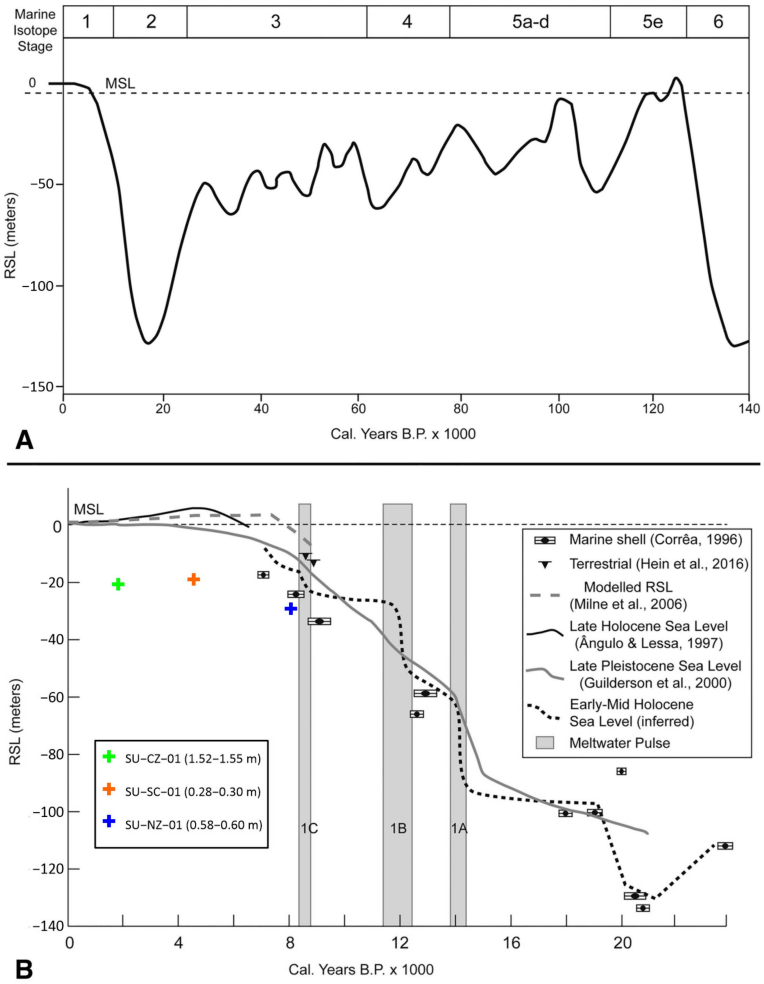

Figure 9. Sea level curves. (**A**) Global eustatic curve since last interglacial (MIS 5) (adapted from [88], compiled from various sources). (**B**) Inferred sea level curve for southern Brazil (from [89,90], based

on [91,92]). Meltwater pulse timing based on [93]. Uplift-corrected sea-level curve from the Argentina shelf from [94], with the location of the samples from the Holocene SU-NZ-01, SU-CZ-01 and SU-SZ-01 seismic units (depth against age of formation). Datum is MSL. The location of the CZ and SZ depocenters near small river mouths explains the subsequent development of SU-CZ-01 and SU-SZ-02 after the Holocene Transgression Maximum (HTM). However, this modern layer has not developed in the NZ due to the absence of significant fluvial inputs. This implies that since the HTM, the input of fine sediments from the São Sebastião Channel has been insufficient to develop notable mud deposition in the NZ depocenter above SU-NZ-01.

Finally, it should be noted that mud deposits linked exclusively to contemporaneous processes are also observed along continental shelves. For instance, a Holocene mud deposit was identified along the continental shelf of the Aquitaine region in France, exclusively associated with a major anthropogenic disturbance near the Gironde Estuary [95]. Modern anthropogenic influences were also observed in the vicinity of the CZ depocenter, particularly near Ponta da Manduba, which received substantial amounts of material from dredging activities in the Santos harbor channel between the 1960s and 1980s [96]. These anthropic activities may have contributed to the supply of muddy sediments in the region; however, the age and thickness of the three depocenters identified in the present study suggest that their influence is minimal and confined to the uppermost portion of the sedimentary record.

5. Conclusions

The central portion of the São Paulo Bight receives a limited supply of modern sediment due to the absence of significant fluvial systems, resulting in a predominance of relict sandy sediment in the region. However, three Holocene mud depocenters have developed near the São Sebastião Channel, the Santos Estuary, and the Peruíbe River mouth. These mud deposits contain a blend of sand, silt, and clay, with silt content systematically higher than that of clay content.

The central depocenter near Moela Island comprises an older sedimentary unit (SU-CZ-02) and a more recent one (SU-CZ-01), coexisting within the central part of this depocenter. SU-CZ-01 generally has a higher mean thickness (5.2 $\pm$ 1.3 m) compared to SU-CZ-02 (0.8 $\pm$ 1.2 m). In contrast, the northern depocenter, near the island of Montão de Trigo, is characterized by a single sedimentary unit, SU-NZ-01, with an average thickness of 5.2 $\pm$ 1.1 m. The southern depocenter, with an estimated total thickness of about 15 m, is composed of two sedimentary units: a thinner, superficial layer of coarser sediments (SU-SZ-01) and a thicker, basal layer of finer sediments (SU-SZ-02). The location and thickness of these three depocenters are influenced by the presence of Precambrian rock surfaces, which created wave shadow zones and trapped sediments within paleovalleys. All three mud depocenters are located within a consistent bathymetric range (shallower than 30 m depth), aligning with the occurrence of the PRS in both outcrops and shallow subcrops.

The lower sedimentary units of depocenters CZ (SU-CZ-02) and SZ (SU-SZ-02), as well as the single sedimentary unit of depocenter NZ (SU-NZ-01), were deposited during the Holocene transgression, prior to the HTM. These units include reworked sediments from the Pleistocene coastal plains that fill the irregular relief of the PRS, characterized by a transparent seismic pattern. Above these, new units formed in the CZ (SU-CZ-01) and SZ (SU-SZ-01) depocenters post-HTM, associated with the input of mud from the Santos Estuary and Peruíbe River, respectively. A second sedimentary unit did not develop in the NZ depocenter, suggesting a lack of significant mud input from any river or the São Sebastião Channel since the HTM.

Author Contributions: Conceptualization, J.A.-C.; Methodology, J.A.-C. and A.S.N.; Validation, A.S.N. and J.A.-C.; Formal Analysis, A.S.N. and J.A.-C.; Investigation, A.S.N. and J.A.-C.; Resources, J.A.-C.; Data Curation J.A.-C. and A.S.N.; Writing—Original Draft Preparation, A.S.N. and J.A.-C.; Writing—Review and Editing, J.A.-C. and A.S.N.; Visualization, A.S.N. and J.A.-C.; Supervision, J.A.-C. All authors have read and agreed to the published version of the manuscript.

Funding: This study is a contribution to the research project "Hydrodynamic and geomorphologic control of muddy deposits in the inner continental shelf (Peruíbe–São Sebastião sectors, SE of Brazil)" (HIGEOLAP, ref. 2015/16067-2), funded by the Fundação de Amparo à Pesquisa do Estado de São Paulo (FAPESP). J.A.-C. gratefully acknowledges the grant "Ayudas para la Recualificación del Sistema Universitario Español" ref. CA2/RSUE/2021-00418.

Institutional Review Board Statement: Not applicable.

Informed Consent Statement: Not applicable.

Data Availability Statement: The original contributions presented in the study are included in the article; further inquiries can be directed to the corresponding author.

Acknowledgments: The authors thank Michel Mahiques for providing the geophysical equipment, as well as the staff of the Alpha Delphini Oceanographic Vessel of the Instituto Oceanográfico of the University of São Paulo for their collaboration in the geophysical surveys, and the Diretoria de Hidrografia e Navegação (Brazilian Navy) for providing data of grain size curves and carbonate content of surface sediment samples. The authors thank the anonymous reviewers for their comments, which contributed significantly to improving the final version of the manuscript.

Conflicts of Interest: The author Antonio Scardua Neto was employed by the company EGS Brasil. The remaining author declares that the research was conducted in the absence of any commercial or financial relationships that could be construed as a potential conflict of interest.

References

1. Walsh, J.P.; Nittrouer, C.A. Understanding Fine-Grained River-Sediment Dispersal on Continental Margins. *Mar. Geol.* **2009**, *263*, 34–45. [CrossRef]
2. Meade, R.H. Chapter 3: River-Sediment Inputs to Major Deltas. In *Sea Level-Rise and Coastal Subsidence*; Springer: Dordrecht, The Netherlands, 1996. [CrossRef]
3. Wells, J.T.; Coleman, J.M. Longshore Transport of Mud by Waves: Northeastern Coast of South America. *Geol. Min.* **1978**, *57*, 353–359.
4. Curtin, T.B. Physical Observations in the Plume Region of the Amazon River during Peak Discharge-III. Currents. *Cont. Shelf Res.* **1986**, *6*, 73–86. [CrossRef]
5. Lentz, S.J. Seasonal Variations in the Horizontal Structure of the Amazon Plume Inferred from Historical Hydrographic Data. *J. Geophys. Res.* **1995**, *100*, 2391–2400. [CrossRef]
6. Hanebuth, T.J.J.; Lantzsch, H. A Late Quaternary Sedimentary Shelf System under Hyperarid Conditions: Unravelling Climatic, Oceanographic and Sea-Level Controls (Golfe d'Arguin, Mauritania, NW Africa). *Mar. Geol.* **2008**, *256*, 77–89. [CrossRef]
7. Lantzsch, H.; Hanebuth, T.J.J.; Bender, V.B. Holocene Evolution of Mud Depocentres on a High-Energy, Low-Accumulation Shelf (NW Iberia). *Quat. Res.* **2009**, *72*, 325–336. [CrossRef]
8. Stow, D.V.; Bowen, A.J. A Physical Model for the Transport and Sorting of Fine-grained Sediment by Turbidity Currents. *Sedimentology* **1980**, *27*, 31–46. [CrossRef]
9. Swift, D.J.P. Quaternary Shelves and the Return to Grade. *Mar. Geol.* **1970**, *8*, 5–30. [CrossRef]
10. Mccave, I.N. Transport and Escape of Fine-Grained Sediment from Shelf Areas. In *Shelf Sediment Transport*; Swift, D.J.P., Duane, D., Pilkey, O.H., Eds.; Dowden, Hutchinson & Ross: Stroudsburg, PA, USA, 1972; pp. 225–248. [CrossRef]
11. Hanebuth, T.J.J.; Lantzsch, H.; Nizou, J. Mud Depocenters on Continental Shelves—Appearance, Initiation Times, and Growth Dynamics. *Geo-Marine Lett.* **2015**, *35*, 487–503. [CrossRef]
12. Hartwell, S.I. Distribution of DDT and Other Persistent Organic Contaminants in Canyons and on the Continental Shelf off the Central California Coast. *Mar. Environ. Res.* **2008**, *65*, 199–217. [CrossRef]
13. Liu, S.; Shi, X.; Liu, Y.; Zhu, Z.; Yang, G.; Zhu, A.; Gao, J. Concentration Distribution and Assessment of Heavy Metals in Sediments of Mud Area from Inner Continental Shelf of the East China Sea. *Environ. Earth Sci.* **2011**, *64*, 567–579. [CrossRef]
14. De Mahiques, M.M.; Hanebuth, T.J.J.; Martins, C.C.; Montoya-Montes, I.; Alcántara-Carrió, J.; Figueira, R.C.L.; Bícego, M.C. Mud Depocentres on the Continental Shelf: A Neglected Sink for Anthropogenic Contaminants from the Coastal Zone. *Environ. Earth Sci.* **2016**, *75*, 44. [CrossRef]
15. Vallejo Toro, P.P.; Vásquez Bedoya, L.F.; Correa, I.D.; Bernal Franco, G.R.; Alcántara-Carrió, J.; Palacio Baena, J.A. Impact of Terrestrial Mining and Intensive Agriculture in Pollution of Estuarine Surface Sediments: Spatial Distribution of Trace Metals in the Gulf of Urabá, Colombia. *Mar. Pollut. Bull.* **2016**, *111*, 311–320. [CrossRef]
16. Hanebuth, T.J.J.; King, M.L.; Mendes, I.; Lebreiro, S.; Lobo, F.J.; Oberle, F.K.; Antón, L.; Ferreira, P.A.; Reguera, M.I. Hazard Potential of Widespread but Hidden Historic Offshore Heavy Metal (Pb, Zn) Contamination (Gulf of Cadiz, Spain). *Sci. Total Environ.* **2018**, *637–638*, 561–576. [CrossRef] [PubMed]
17. Lesueur, P.; Jouanneau, J.M.; Boust, D.; Tastet, J.P.; Weber, O. Sedimentation Rates and Fluxes in the Continental Shelf Mud Fields in the Bay of Biscay (France). *Cont. Shelf Res.* **2001**, *21*, 1383–1401. [CrossRef]

18. Calliari, L.J.; Holland, K.T.; Pereira, P.S.; Guedes, R.M.C.; Santo, R.E. The Influence of Mud on the Inner Shelf, Shoreface, Beach and Surf Zone Morphodynamics—Cassino, Southern Brazil. In Proceedings of the 6th International Symposium on Coastal Engineering and Science of Coastal Sediment Processes, New Orleans, LA, USA, 13–17 May 2007; pp. 1455–1465. [CrossRef]
19. Sommerfield, C.K.; Wheatcroft, R.A. Late Holocene Sediment Accumulation on the Northern California Shelf: Oceanic, Fluvial, and Anthropogenic Influences. *Geol. Soc. Am. Bull.* **2007**, *119*, 1120–1134. [CrossRef]
20. Bernárdez, P.; González-Álvarez, R.; Francés, G.; Prego, R.; Bárcena, M.A.; Romero, O.E. Palaeoproductivity Changes and Upwelling Variability in the Galicia Mud Patch during the Last 5000 Years: Geochemical and Microfloral Evidence. *Holocene* **2008**, *18*, 1207–1218. [CrossRef]
21. Liu, J.T.; Hsu, R.T.; Yang, R.J.; Wang, Y.P.; Wu, H.; Du, X.; Li, A.; Chien, S.C.; Lee, J.; Yang, S.; et al. A Comprehensive Sediment Dynamics Study of a Major Mud Belt System on the Inner Shelf along an Energetic Coast. *Sci. Rep.* **2018**, *8*, 4229. [CrossRef]
22. Nizou, J.; Dennielou, B.; Révillon, S.; Bassetti, M.A.; Jouet, G.; Berné, S.; Nonnotte, P.; Liorzou, C. Records of Holocene Climatic Fluctuations and Anthropogenic Lead Input in Elemental Distribution and Radiogenic Isotopes (Nd and Pb) in Sediments of the Gulf of Lions (Southern France). *Holocene* **2019**, *29*, 1292–1304. [CrossRef]
23. Zembruscki, S.G. Geomorfologia Da Margem Continental Sul Brasileira e Das Bacias Oceânicas Adjacentes. In *Geomorfologia da Margem Continental Brasileira e Áreas Oceânicas Adjacentes*; Chaves, H.A.F., Ed.; Petrobras: Rio de Janeiro, Brazil, 1979; pp. 129–177.
24. De Mahiques, M.M.; de Mello e Sousa, S.H.; Furtado, V.V.; Tessler, M.G.; de Lima Toledo, F.A.; Burone, L.; Figueira, R.C.L.; Klein, D.A.; Martins, C.C.; Alves, D.P.V. The Southern Brazilian Shelf: General Characteristics, Quaternary Evolution and Sediment Distribution. *Brazilian J. Oceanogr.* **2010**, *58*, 25–34. [CrossRef]
25. Almeida, F.F.M. The System of Continental Rifts Bordering the Santos Basin, Brazil. *An. Acad. Bras. Cienc.* **1976**, *48*, 15–26.
26. Kowsmann, R.O.; Costa, M.P.A.; Vicalvi, M.A.; Coutinho, M.G.N.; Gamboa, L.P.A. Modelo Da Sedimentação Holocênica Na Plataforma Continental Sul Brasileira. In *Evolução Sedimentar Holocênica da Plataforma Continental e do Talude do Sul do Brasil*; Série Projeto REMAC: Rio de Janeiro, Brazil, 1977; pp. 7–26.
27. Suguio, K.; Martin, L. Formações Quaternárias Marinhas Do Litoral Paulista e Sul Fluminense (Quaternary Marine Formations of the State of São Paulo and Southern Rio de Janeiro). In Proceedings of the 1978 International Symposium on Coastal Evolution in the Quaternary, São Paulo, Brazil, 11–18 September 1978; pp. 1–55.
28. Conti, L.A.; Furtado, V.V. Geomorfologia Da Plataforma Continental Do Estado De São Paulo. *Rev. Bras. Geociências* **2006**, *36*, 305–312. [CrossRef]
29. De Mahiques, M.M.; Tessler, M.G.; Maria Ciotti, A.; Da Silveira, I.C.A.; E Sousa, S.H.D.M.; Figueira, R.C.L.; Tassinari, C.C.G.; Furtado, V.V.; Passos, R.F. Hydrodynamically Driven Patterns of Recent Sedimentation in the Shelf and Upper Slope off Southeast Brazil. *Cont. Shelf Res.* **2004**, *24*, 1685–1697. [CrossRef]
30. Mahiques, M.M.; Sousa, S.H.M.; Burone, L.; Nagai, R.H.; Silveira, I.C.A.; Figueira, R.C.L.; Soutelino, R.G.; Ponsoni, L.; Klein, D.A. Radiocarbon Geochronology of the Sediments of the São Paulo Bight (Southern Brazilian Upper Margin). *An. Acad. Bras. Cienc.* **2011**, *83*, 817–834. [CrossRef] [PubMed]
31. De Mahiques, M.M.; Mishima, Y.; Rodrigues, M. Characteristics of the Sedimentary Organic Matter on the Inner and Middle Continental Shelf between Guanabara Bay and Sao Francisco Do Sul, Southeastern Brazilian Margin. *Cont. Shelf Res.* **1999**, *19*, 775–798. [CrossRef]
32. Rodrigues, M.; Furtado, V.V.; Tessler, M.G.; Mahiques, M.M. *Atlas Sedimentológico Da Plataforma Continental Do Estado de São Paulo: Texto Explicativo e Mapas*; Instituto Oceanografico Universidade de Sao Paulo: Sao Paulo, Brazil, 2001.
33. Figueiredo, A.G.; Tessler, M.G. *Topografia e Composição Do Substrato Marinho Da Região Sudeste-Sul Do Brasil*; Instituto Oceanográfico Universidade de São Paulo, Série Documentos REVIZEE—Score Sul: São Paulo, Brazil, 2004.
34. Silva, J.F. Dados Climatológicos de Cananéia e Ubatuba (Estado de São Paulo). *Bol. Clim. do Inst. Ocean.* **1989**, *6*, 1–21.
35. Cerda, C.; Castro, B.M. Hydrographic Climatology of South Brazil Bight Shelf Waters between Sao Sebastiao (24°S) and Cabo Sao Tome (22°S). *Cont. Shelf Res.* **2014**, *89*, 5–14. [CrossRef]
36. De Castro Filho, B.M.; de Miranda, L.B.; Miyao, S.Y. Condições Hidrográficas Na Plataforma Continental Ao Largo de Ubatuba: Variações Sazonais e Em Média Escala. *Bol. do Inst. Ocean.* **1987**, *35*, 135–151. [CrossRef]
37. Pianca, C.; Mazzini, P.L.F.; Siegle, E. Brazilian Offshore Wave Climate Based on NWW3 Reanalysis. *Brazilian J. Oceanogr.* **2010**, *58*, 53–70. [CrossRef]
38. Mesquita, A.R.; Harari, J. *Tides and Tide Gauges of Cananéia and Ubatuba-Brazil (Lat. 24°)*; Internal Report Oceanographic Institute of São Paulo: São Paulo, Brazil, 1983.
39. Dottori, M.; Castro, B.M. The Response of the Sao Paulo Continental Shelf, Brazil, to Synoptic Winds. *Ocean Dyn.* **2009**, *59*, 603–614. [CrossRef]
40. Blott, S.J.; Pye, K. GRADISTAT: A Grain Size Distribution and Statistics Package for the Analysis of Unconsolidated Sediments. *Estuar. Coast. Shelf Sci.* **2001**, *26*, 1237–1248. [CrossRef]
41. Folk, R.L.; Ward, W.C. Brazos River Bar [Texas]; a Study in the Significance of Grain Size Parameters. *J. Sediment. Res.* **1957**, *27*, 3–26. [CrossRef]
42. Navarra, C.T.; Furtado, V.V.; Eichler, B.B.; Prado, O.R. do Distribuição Da Matéria Orgânica Nos Sedimentos Marinhos Costeiros e Nos Solos Hidromórficos Da Orla Litorânea Do Estado de São Paulo. *Brazilian J. Oceanogr.* **1980**, *29*, 267–270. [CrossRef]
43. Ingram, R.L. Sieve Analysis. In *Procedures in Sedimentary Petrology*; Carver, R.E., Ed.; Wiley-Interscience: New York, NY, USA, 1971; pp. 49–67.

44. Suguio, K. *Introdução à Sedimentologia*; Blücher, E., Ed.; Editorial Universidade Sao Paulo: São Paulo, Brazil, 1973.
45. Folk, R.L. The Distinction between Grain Size and Mineral Composition in Sedimentary-Rock Nomenclature. *J. Geol.* **1954**, *62*, 344–359. [CrossRef]
46. Alves, E.; Macario, K.; Souza, R.; Pimenta, A.; Douka, K.; Oliveira, F.; Chanca, I.; Angulo, R. Radiocarbon Reservoir Corrections on the Brazilian Coast from Pre-Bomb Marine Shells. *Quat. Geochronol.* **2015**, *29*, 30–35. [CrossRef]
47. Reimer, P.J.; Bard, E.; Bayliss, A.; Beck, J.W.; Blackwell, P.G.; Ramsey, C.B.; Buck, C.E.; Cheng, H.; Edwards, R.L.; Friedrich, M.; et al. IntCal13 and Marine13 Radiocarbon Age Calibration Curves 0–50,000 Years Cal BP. *Radiocarbon* **2013**, *55*, 1869–1887. [CrossRef]
48. Kowsmann, R.O.; Costa, M.P.A. Paleolinhas de Cota Na Plataforma Continental Das Regiões Sul e Norte Brasileira. *Rev. Bras. Geociências* **1974**, *4*, 215–222.
49. Da Rocha, J.; Milliman, J.D.; Santana, C.I.; Vicalvi, M.A.; Füchtbauer, H.; Lisitzyn, A.P.; Milliman, J.D.; Seibold, E. Southern Brazil. In *Upper Continental Margin Sedimentation off Brazil 4*; Milliman, J.D., Summerhayes, C.P., Eds.; Schweizerbart: Stuttgart, Germany, 1975; pp. 117–150.
50. Corrêa, I.C.S. Distribuição Dos Sedimentos Modernos Da Plataforma Continental Entre São Paulo e Santa Catarina. *Pesqui. em Geociências* **1980**, *13*, 109. [CrossRef]
51. Furtado, V.V.; Tessler, M.G.; Eichler, B.B. Distribuição de Sedimentos de Fundo Na Plataforma Continental de São Paulo. In Proceedings of the Simpósio Brasileiro Sobre os Recursos do mar, Rio de Janeiro, Brazil, 5–7 November 1984; p. 15.
52. Furtado, V.V.; Mahiques, M.M. Distribuição de Sedimentos Em Regiões Costeiras e Plataforma Continental Norte Do Estado de São Paulo. In Proceedings of the Simpósio de Ecossistemas da Costa Sul e Sudeste Brasileira, Estrutura, Função e Manejo, Águas de Lindóia, Brazil, 2–7 April 1990; pp. 20–29.
53. De Mahiques, M.M.; Da Silveira, I.C.A.; De Mello e Sousa, S.H.; Rodrigues, M. Post-LGM Sedimentation on the Outer Shelf-Upper Slope of the Northernmost Part of the São Paulo Bight, Southeastern Brazil. *Mar. Geol.* **2002**, *181*, 387–400. [CrossRef]
54. Yokoyama, C.J. Mobilidade Sedimentar Da Plataforma Continental Do Estado de São Paulo Em Função Da Propagação de Ondas. Master's Thesis, University of São Paulo, São Paulo, Brazil, 2013.
55. Martins, L.R.; Coutinho, P.N. The Brazilian Continental Margin. *Earth Sci. Rev.* **1981**, *17*, 87–107. [CrossRef]
56. Martins, L.R.; Urien, C.M.; Butler, L.W.; Martins, J.R. Morfologia e Sedimentos Da Plataforma Continental Atlântica Sul-Americana Entre Cabo Orange e Chui (Brasil). *An. Hidrográficos* **1975**, *32*, 83–109.
57. Nittrouer, C.A.; Kuehl, S.A.; Demaster, D.J.; Kowsmann, R.O. The Deltaic Nature of Amazon Shelf Sedimentation. *Geol. Soc. Am. Bull.* **1986**, *97*, 444–458. [CrossRef]
58. Patchineelam, S.R.; Smoak, J.M. Sediment Accumulation Rates along the Inner Eastern Brazilian Continental Shelf. *Geo-Marine Lett.* **1999**, *19*, 196–201. [CrossRef]
59. Vieira, I.; Lobo, F.J.; Montoya-Montes, I.; Siegle, E.; Passos, J.L.; De Mahiques, M.M. A Non-Deltaic Clinoform Wedge Fed by Multiple Sources off São Sebastião Island, Southeastern Brazilian Shelf. *Geo-Marine Lett.* **2018**, *38*, 63–81. [CrossRef]
60. Guerrero, R.A.; Acha, E.M.; Framiñan, M.B.; Lasta, C.A. Physical Oceanography of the Río de La Plata Estuary, Argentina. *Cont. Shelf Res.* **1997**, *17*, 727–742. [CrossRef]
61. Luiz, E.S.L.; de Oliveira, A. Análise de Vazões Da Bacia Hidrográfica Do Rio Paraíba Do Sul, Variabilidades, Intensidades e Períodos de Retorno. In *Os Desafios da Geografia Física na Fronteira do Conhecimento*; UNICAMP: Campinas, Brazil, 2017; pp. 1857–1864. [CrossRef]
62. Liu, Y.; Gao, S.; Wang, Y.P.; Yang, Y.; Long, J.; Zhang, Y.; Wu, X. Distal Mud Deposits Associated with the Pearl River over the Northwestern Continental Shelf of the South China Sea. *Mar. Geol.* **2014**, *347*, 43–57. [CrossRef]
63. Dias, J.M.A.; Boski, T.; Rodrigues, A.; Magalhães, F. Coast Line Evolution in Portugal since the Last Glacial Maximum until Present—A Synthesis. *Mar. Geol.* **2000**, *170*, 177–186. [CrossRef]
64. Kuehl, S.A.; Nittrouer, C.A.; Allison, M.A.; Faria, L.E.C.; Dukat, D.A.; Jaeger, J.M.; Pacioni, T.D.; Figueiredo, A.G.; Underkoffler, E.C. Sediment Deposition, Accumulation, and Seabed Dynamics in an Energetic Fine-Grained Coastal Environment. *Cont. Shelf Res.* **1996**, *16*, 787–815. [CrossRef]
65. Lantzsch, H.; Hanebuth, T.J.J.; Chiessi, C.M.; Schwenk, T.; Violante, R.A. The High-Supply, Current-Dominated Continental Margin of Southeastern South America during the Late Quaternary. *Quat. Res.* **2014**, *81*, 339–354. [CrossRef]
66. Dubrulle, C.; Jouanneau, J.M.; Lesueur, P.; Bourillet, J.F.; Weber, O. Nature and Rates of Fine-Sedimentation on a Mid-Shelf: "La Grande Vasière" (Bay of Biscay, France). *Cont. Shelf Res.* **2007**, *27*, 2099–2115. [CrossRef]
67. Larsonneur, C.; Bouysse, P.A.; Auffret, J.P. The Superficial Sediments of the English Channel and Its Western Approaches. *Sedimentology* **1982**, *29*, 851–864. [CrossRef]
68. Lobo, F.J.; Sánchez, R.; González, R.; Dias, J.M.A.; Hernández-Molina, F.J.; Fernández-Salas, L.M.; Díaz Del Río, V.; Mendes, I. Contrasting Styles of the Holocene Highstand Sedimentation and Sediment Dispersal Systems in the Northern Shelf of the Gulf of Cadiz. *Cont. Shelf Res.* **2004**, *24*, 461–482. [CrossRef]
69. Crockett, J.S.; Nittrouer, C.A.; Ogston, A.S.; Goni, M.A. *Chapter 5 Variable Styles of Sediment Accumulation Impacting Strata Formation on a Clinoform: Gulf of Papua, Papua New Guinea*; Elsevier B.V.: Amsterdam, The Netherlands, 2008; Volume 9, ISBN 9780444529640.
70. Nizou, J.; Hanebuth, T.J.J.; Heslop, D.; Schwenk, T.; Palamenghi, L.; Stuut, J.B.; Henrich, R. The Senegal River Mud Belt: A High-Resolution Archive of Paleoclimatic Change and Coastal Evolution. *Mar. Geol.* **2010**, *278*, 150–164. [CrossRef]

71. Xu, K.; Li, A.; Liu, J.P.; Milliman, J.D.; Yang, Z.; Liu, C.S.; Kao, S.J.; Wan, S.; Xu, F. Provenance, Structure, and Formation of the Mud Wedge along Inner Continental Shelf of the East China Sea: A Synthesis of the Yangtze Dispersal System. *Mar. Geol.* **2012**, *291–294*, 176–191. [CrossRef]
72. Milliman, J.D.; Meade, R.H. World-Wide Delivery of River Sediment to the Oceans. *J. Geol.* **1983**, *91*, 1–21. [CrossRef]
73. Alcántara-Carrió, J.; Mahiques, M.M.; Cazzoli y Goya, S.; Fontán-Bouzas, A. Sedimentary Dynamics of a Subtropical Tidal Flat Sheltered inside a Coastal Channel (Araçá Bay, SE Brazil). *Ocean Coast. Manag.* **2018**, *164*, 32–41. [CrossRef]
74. Alcántara-Carrió, J.; Sasaki, D.K.; de Mahiques, M.M.; Taborda, R.; de Souza, L.A.P. Sedimentary Constraints on the Development of a Narrow Deep Strait (São Sebastião Channel, SE Brazil). *Geo-Marine Lett.* **2017**, *37*, 475–488. [CrossRef]
75. Coelho, T.M. Análise Do Transporte de Sedimentos Na Região Central Da Baixada Santista (SP) Através de Modelagem Numérica. Master's Thesis, Universidade de São Paulo, São Paulo, Brazil, 2011.
76. Tyson, R.V. *Sedimentary Organic Matter: Organic Facies and Palynofacies*; Chapman & Hall: London, UK, 1995.
77. Siqueira, G.; Braga, E.; Mahíques, M.; Aprile, F. Determinação Da Matéria Orgânica E Razões C-N. *Arq. Ciências Mar* **2006**, *39*, 18–27.
78. Kim, B.S.M.; Bícego, M.C.; Taniguchi, S.; Siegle, E.; Oliveira, R.; Alcántara-Carrió, J.; Figueira, R.C.L. Organic and Inorganic Contamination in Sediments from Araçá Bay, São Sebastião, Brazil. *Ocean Coast. Manag.* **2018**, *164*, 42–51. [CrossRef]
79. Burone, L.; Muniz, P.; Pires-vanin, A.N.A.M.S. Spatial Distribution of Organic Matter in the Surface Sediments of Ubatuba Bay (Southeastern—Brazil). *An. Acad. Bras. Cienc.* **2003**, *75*, 77–90. [CrossRef]
80. Drago, T.; Araújo, F.; Valério, P.; Weber, O.; Jouanneau, J.M. Geomorphological Control of Fine Sedimentation on the Northern Portuguese Shelf. *Boletín Inst. Español Oceanogr.* **1999**, *15*, 111–122.
81. Gyllencreutz, R.; Jakobsson, M.; Backman, J. Holocene Sedimentation in the Skagerrak Interpreted from Chirp Sonar and Core Data. *J. Quat. Sci.* **2005**, *20*, 21–32. [CrossRef]
82. Dias, G.T.M. Baía de Guanabara—Fáceis Sedimentares Superficias. Sismo Estratigrafia. In Proceedings of the Resumo 1o Congresso Sociedade Brasileira de Geofisica, Rio de Janeiro, Brazil, 1–6 October 1989.
83. Nordfjord, S.; Goff, J.A.; Austin, J.A.; Gulick, S.P.S. Seismic Facies of Incised-Valley Fills, New Jersey Continental Shelf: Implications for Erosion and Preservation Processes Acting during Latest Pleistocene-Holocene Transgression. *J. Sediment. Res.* **2006**, *76*, 1284–1303. [CrossRef]
84. Fernández-Salas, L.M.; Lobo, F.J.; Hernández-Molina, F.J.; Somoza, L.; Rodero, J.; Díaz Del Río, V.; Maldonado, A. High-Resolution Architecture of Late Holocene Highstand Prodeltaic Deposits from Southern Spain: The Imprint of High-Frequency Climatic and Relative Sea-Level Changes. *Cont. Shelf Res.* **2003**, *23*, 1037–1054. [CrossRef]
85. Dung, B.V.; Stattegger, K.; Unverricht, D.; Van Phach, P.; Thanh, N.T. Late Pleistocene-Holocene Seismic Stratigraphy of the Southeast Vietnam Shelf. *Glob. Planet. Change* **2013**, *110*, 156–169. [CrossRef]
86. Aquino da Silva, A.G.; Stattegger, K.; Schwarzer, K.; Vital, H. Seismic Stratigraphy as Indicator of Late Pleistocene and Holocene Sea Level Changes on the NE Brazilian Continental Shelf. *J. South Am. Earth Sci.* **2016**, *70*, 188–197. [CrossRef]
87. Cooper, J.A.G.; Green, A.N.; Meireles, R.; Klein, A.H.F.; de Abreu, J.G.N.; Toldo, E.E. Tidal Strait to Embayment: Seismic Stratigraphy and Evolution of a Rock-Bounded Embayment in the Context of Holocene Sea Level Change. *Mar. Geol.* **2019**, *415*, 105972. [CrossRef]
88. Bailey, G.N.; Flemming, N.C.; King, G.C.P.; Lambeck, K.; Momber, G.; Moran, L.J.; Al-Sharek, A.; Vita-Finzi, A. Coastlines, Submerged Landscapes, and Human Evolution: The Red Sea Basin and the Farasan Islands. *J. Isl. Coast. Archaeol.* **2007**, *2*, 127–160. [CrossRef]
89. Cooper, J.A.G.; Green, A.N.; Meireles, R.P.; Klein, A.H.F.; Souza, J.; Toldo, E.E. Sandy Barrier Overstepping and Preservation Linked to Rapid Sea Level Rise and Geological Setting. *Mar. Geol.* **2016**, *382*, 80–91. [CrossRef]
90. Cooper, J.A.G.; Meireles, R.P.; Green, A.N.; Klein, A.H.F.; Toldo, E.E. Late Quaternary Stratigraphic Evolution of the Inner Continental Shelf in Response to Sea-Level Change, Santa Catarina, Brazil. *Mar. Geol.* **2018**, *397*, 1–14. [CrossRef]
91. Corrêa, I.C.S. Les Variations Du Niveau de La Mer Durant Les Derniers 17.500 Ans BP: L'exemple de La Plate-Forme Continentale Du Rio Grande Do Sul-Brésil. *Mar. Geol.* **1996**, *130*, 163–178. [CrossRef]
92. Angulo, R.J.; Lessa, G.C. The Brazilian Sea-Level Curves: A Critical Review with Emphasis on the Curves from the Paranagua and Cananeia Regions. *Mar. Geol.* **1997**, *140*, 141–166. [CrossRef]
93. Liu, J.P.; Milliman, J.D. Reconsidering Melt-Water Pulses 1A and 1B: Global Impacts of Rapid Sea-Level Rise. *J. Ocean Univ. China* **2004**, *3*, 183–190. [CrossRef]
94. Guilderson, T.P.; Burckle, L.; Hemming, S.; Peltier, W.R. Late Pleistocene Sea Level Variations Derived from the Argentina Shelf. *Geochemistry, Geophys. Geosystems* **2000**, *1*, 1–14. [CrossRef]
95. Lesueur, P.; Tastet, J.P.; Marambat, L. Shelf Mud Fields Formation within Historical Times: Examples from Offshore the Gironde Estuary, France. *Cont. Shelf Res.* **1996**, *16*, 1849–1870. [CrossRef]
96. Rocha, A.C. Aplicação de Métodos Diretos e Indiretos Na Análise de Sedimentos Na Baía de Santos—SP. Master's Thesis, University of São Paulo, São Paulo, Brazil, 2003.